GE Research &
Development Center

A High-Performance Reduced-Complexity GMSK Demodulator

N. Al-Dhahir and G. Saulnier

96CRD107, September 1996
Class 1

Technical Information Series

Corporate Research and Development

Technical Report Abstract Page

Title	A High-Performance Reduced-Complexity GMSK Demodulator		
Author(s)	N. Al-Dhahir G. Saulnier	**Phone**	(518)387-7092 8*833-7092
Component	Electronic Systems Laboratory		
Report Number	96CRD107	**Date**	September 1996
Number of Pages	12	**Class**	1
Key Words	Gaussian minimum shift keying, Viterbi algorithm , intersymbol interference, differential encoding		

A four--state adaptive maximum--likelihood sequence estimator demodulator for GMSK modulation (BT=0.3) on AWGN channels is analyzed and simulated. This demodulator utilizes a linear representation of GMSK signals and achieves the same BER performance as MSK. The channel impulse response used in the MLSE branch metric calculations is derived in closed form and adapted in a decision--directed mode to offset any performance losses incurred by retaining only one term in the linear representation.

Manuscript received July 8, 1996

A High-Performance Reduced-Complexity GMSK Demodulator

Naofal Al-Dhahir and Gary Saulnier

1 Introduction

Gaussian minimum shift keying (GMSK) has been adopted as the digital modulation scheme for the European global system for mobile communications (GSM) standard due to its spectral efficiency and constant–envelope property [5, 6]. These two characteristics result in superior performance in the presence of adjacent channel interference (ACI) and non–linear amplifiers.

Since a GMSK signal is obtained from an MSK signal by prefiltering it with a narrow–band Gaussian filter, it can likewise be interpreted as a special case of continuous–phase frequency shift keying (CPFSK) with a modulation index of 0.5 or as filtered offset quadrature phase shift keying (OQPSK). Therefore, a GMSK signal can be demodulated either differentially or coherently [1] depending on the performance/complexity requirements. In this report, we operate under low $\frac{E_b}{N_0}$ conditions (between 1 and 3 dB), therefore, we assume coherent demodulation due to its lower $\frac{E_b}{N_0}$ requirements compared to differential demodulation for the same bit error rate (BER). The Gaussian pre–filter in GMSK modulation introduces intersymbol interference (ISI) that spreads over several bit intervals, thus, degrading performance from MSK when coherent symbol–by–symbol detection is used [5]. Maximum likelihood sequence estimation (MLSE) using the Viterbi algorithm is well known to achieve optimal performance in the presence of ISI [2]. The optimal MLSE demodulator for GMSK requires 4.2^{L-1} (where L is the ISI duration in bit intervals) states [1, 6] on AWGN channels. The presence of severe multipath fading and narrow–band receive filtering (to reduce ACI) further increases the number of states making implementation complexity prohibitively high.

In this report, we present an MLSE GMSK demodulator that requires 2^{L-1} states and achieves the same BER performance as MSK. Following [3], we utilize a linear representation of GMSK signals in terms of basic pulse amplitude modulation (PAM) signals, that was derived in [4], to design our MLSE demodulator. However, our linearized MLSE GMSK demodulator has several advantages over those described in [3, 6], namely

- We use a standard off–the–shelf Viterbi algorithm (VA), that requires 2^{L+1} additions for updating state metrics and 2^L comparisons to select survivor path, with one sample per bit, whereas the VA branch metric computation in [3] is non–standard and 4 samples per bit are used which implies more computations per bit period.

- Our 4 state GMSK demodulator achieves better performance than that of [3] in AWGN by using the adaptive decision–directed least–mean–square (LMS) algorithm to get a better channel impulse response (CIR) estimate taking effect of $h_k(t)$ $(k = 1, 2, 3)$ into account.

- Because of its linearity, our GMSK demodulator can be readily applied to channels with multipath fading simply by increasing the number of states according to the multipath delay spread. The GMSK demodulator described in [6] is nonlinear, therefore, the overall CIR seen by the Viterbi demodulator is not equal to the convolution of the GMSK phase shaping filter and the channel impulse response.

- The Viterbi demodulator in [6] is much more complex; it uses sine and cosine look–up tables to compute the branch metrics and requires 16 states for GMSK with BT=0.3 on AWGN.

The remainder of this report is organized as follows. In Section 2, we derive a closed–form expression for the phase shaping filter of GMSK which is used in Section 3 to compute a linear representation for the GMSK signal. Section 4 describes a reduced–complexity MLSE demodulator based on this linear representation. A factor of 2 reduction in BER is achieved through differential encoding and is described in Section 5. Finally, simulation results are presented in Section 6.

2 GMSK Modulation

In CPFSK modulation, of which GMSK is a member, the information-carrying phase signal has the form

$$\begin{aligned}\phi(t,\alpha) &= 2\pi h_F \int_{-\infty}^{t} \sum_{i=-\infty}^{\infty} \alpha_i g(\tau - iT) d\tau \\ &\stackrel{def}{=} 2\pi h_F \sum_{i=-\infty}^{\infty} \alpha_i q(t - iT)\,,\end{aligned}$$

where h_F is the modulation index (equal to 0.5 for GMSK) and $g(t)$ and $q(t)$ are the frequency and phase shaping filters, respectively. For GMSK, the frequency shaping filter $g(t)$ is the response of a Gaussian filter to binary non-return-to-zero (NRZ) pulses and is given by

$$g(t) = \frac{1}{2T}(Q(\gamma(t - \frac{T}{2})) - Q(\gamma(t + \frac{T}{2})))\,, \tag{1}$$

where $\gamma \stackrel{def}{=} \frac{2\pi B}{\sqrt{\ln(2)}}$, B is the bandwidth of the Gaussian filter, T is the bit period, and $Q(x) \stackrel{def}{=} \frac{1}{\sqrt{2\pi}} \int_x^\infty e^{-\frac{u^2}{2}} du$. Therefore, the phase shaping filter for GMSK is given by

$$\begin{aligned}q(t) &\stackrel{def}{=} \int_{-\infty}^{t} g(\tau) d\tau \\ &= \frac{1}{2} + \frac{1}{2T}((t - \frac{(L+1)T}{2})Q(\gamma(t - \frac{(L+1)T}{2})) - (t - \frac{(L-1)T}{2})Q(\gamma(t - \frac{(L-1)T}{2})) \\ &- \frac{1}{\gamma\sqrt{2\pi}}(e^{-\frac{\gamma^2}{2}(t-\frac{(L+1)T}{2})^2} - e^{-\frac{\gamma^2}{2}(t-\frac{(L-1)T}{2})^2}))\,,\end{aligned}$$

where L is the duration of $g(t)$ in bit periods and is equal to 3 for GMSK with BT=0.3. The phase shaping filter $q(t)$ for GMSK with BT=0.3 is plotted in Figure 1. Sampling $q(t)$ at a rate of $\frac{\eta}{T}$ (where η is the number of samples per bit and is called the oversampling factor), we get

$$\begin{aligned}q_n &= \frac{1}{2}\{1 + (\frac{n}{\eta} - 2)Q((\frac{n}{\eta} - 2)\gamma T) - (\frac{n}{\eta} - 1)Q((\frac{n}{\eta} - 1)\gamma T) \\ &- \frac{1}{\sqrt{2\pi}\gamma T}(e^{-\frac{1}{2}(((\frac{n}{\eta})-2)\gamma T)^2} - e^{-\frac{1}{2}(((\frac{n}{\eta})-1)\gamma T)^2})\}\end{aligned}$$

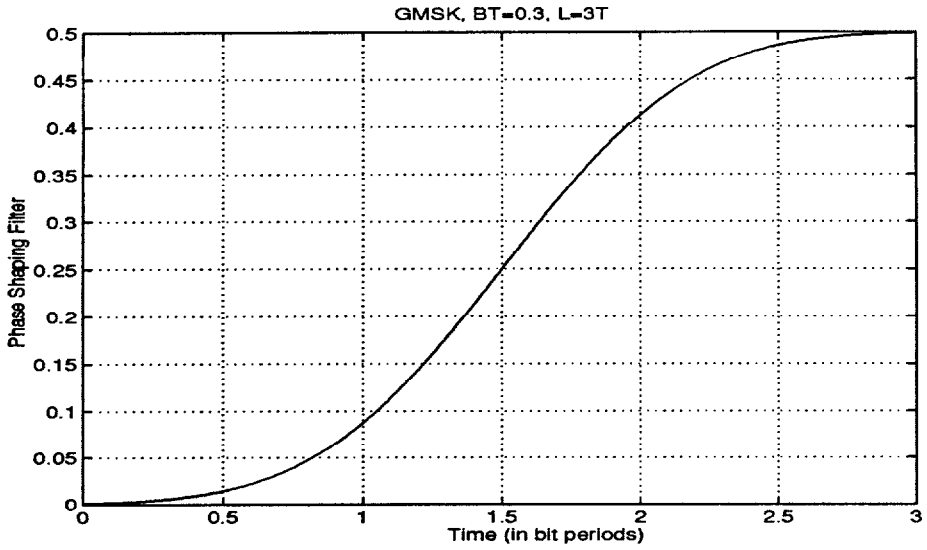

Figure 1: Phase Shaping Filter for GMSK with BT=0.3

$$= \frac{1}{2}\{1 + (\frac{n}{\eta} - 2)Q(2.264(\frac{n}{\eta} - 2)) - (\frac{n}{\eta} - 1)Q(2.264(\frac{n}{\eta} - 1)) - 0.1762(e^{-2.563((\frac{n}{\eta})-2)^2} - e^{-2.563((\frac{n}{\eta})-1)^2})\}$$

In Table 1 we list the coefficients q_n for different values of the oversampling factor η.

η	q_0	q_1	q_2	q_3	q_4	q_5	q_6	q_7	q_8	q_9	q_{10}	q_{11}
1	0.0009	0.0872	0.4128									
2	0.0009	0.0142	0.0872	0.2500	0.4128	0.4858						
3	0.0009	0.0062	0.0290	0.0872	0.1879	0.3121	0.4128	0.4710	0.4938			
4	0.0009	0.0041	0.0142	0.0392	0.0872	0.1603	0.2500	0.3397	0.4128	0.4608	0.4858	0.4959

Table 1: Phase Shaping Filter Coefficients for GMSK with BT= 0.3

3 Linear Approximation of GMSK Signal

It was shown in [4] that any binary continuous phase modulation (CPM) signal with a modulation filter duration L can be expressed as the sum of 2^{L-1} PAM signals. Applying this result to GMSK

with BT=0.3, we can write the transmitted GMSK signal as the sum of four PAM-modulated signals, namely

$$s(t) = \sqrt{\frac{2E_b}{T}} \sum_{k=0}^{3} \sum_{n} j^n a_{k,n} h_k(t - nT) \,, \tag{2}$$

where E_b is the input energy per bit, $j = e^{j\frac{\pi}{2}}$ corresponds to a 90^o phase shift, $a_{k,n} \in \{\pm 1\}$, and

$$\begin{aligned}
h_0(t) &= C(t-3T)C(t-2T)C(t-T) \quad : 0 \le t \le 4T \\
h_1(t) &= C(t-3T)C(t+T)C(t-T) \quad : 0 \le t \le 2T \\
h_2(t) &= C(t-3T)C(t+2T)C(t-2T) \quad : 0 \le t \le T \\
h_3(t) &= C(t-3T)C(t+2T)C(t+T) \quad : 0 \le t \le T \,.
\end{aligned}$$

The basic pulse $C(t)$ is given by [4]

$$C(t) = \begin{cases} \sin(\frac{\pi}{2}(1 - q(t))) & : 0 \le t \le 3T \\ C(-t) & -3T \le t \le 0 \end{cases} .$$

The functions $h_k(t)_{k=0,1,2,3}$ are plotted in Figure 2. We found that $h_0(t)$ contains 99.63% of the total GMSK pulse energy. Therefore, for all practical purposes, we can represent $s(t)$ in terms of $h_0(t)$ only, which would simplify the receiver structure significantly. In other words, we can write

$$\begin{aligned}
s(t) &\approx \sqrt{\frac{2E_b}{T}} \sum_{n} j^n a_{0,n} h_0(t - nT) \\
&\stackrel{def}{=} \sqrt{\frac{2E_b}{T}} \sum_{n} b_n h_0(t - nT) \,,
\end{aligned}$$

where the complex symbols b_n belong to the signal constellation $\{\pm 1, \pm j\}$. The anti-podal symbols $a_{0,n}$ are related to the transmitted anti-podal symbols α_n by the encoding rule $a_{0,n} = \alpha_n a_{0,n-1}$. A block diagram of this linear approximation for the GMSK modulator is given in Figure 3.

In Table 2, we list the coefficients of the main pulse $h_0(t)$ for different values of the oversampling factor η.

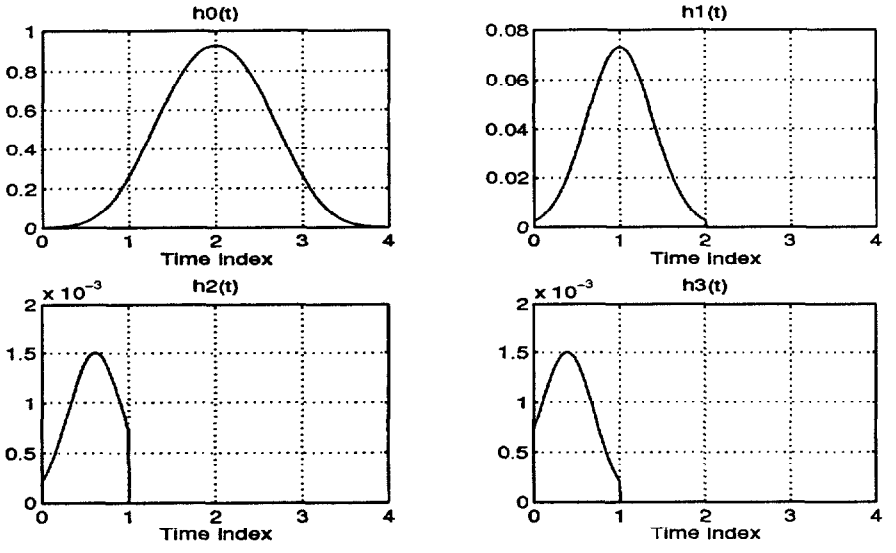

Figure 2: The 4 PAM Pulses Needed for the Linear Representation of GMSK Signals with $BT = 0.3$

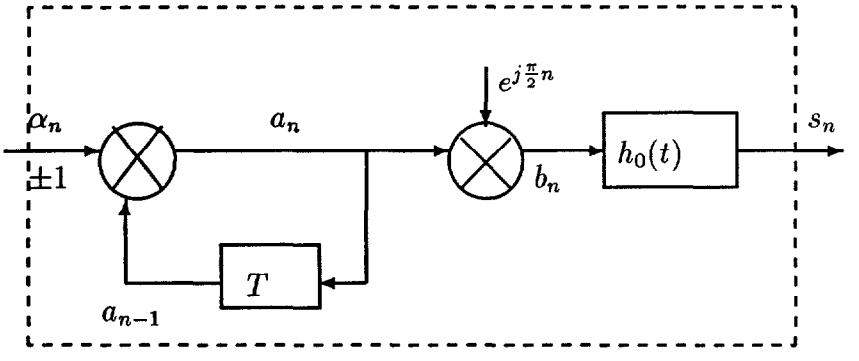

Figure 3: Linear Approximation of GMSK Modulator

η	$h_0(0)$	$h_0(1)$	$h_0(2)$	$h_0(3)$	$h_0(4)$	$h_0(5)$	$h_0(6)$	$h_0(7)$	$h_0(8)$	$h_0(9)$	$h_0(10)$	$h_0(11)$	$h_0(12)$	$h_0(13)$
1	0.0007	0.2605	0.9268	0.2605	0.0007									
2	0.0007	0.0315	0.2605	0.7057	0.9268	0.7057	0.2605	0.0315						
3	0.0007	0.0108	0.0756	0.2605	0.5542	0.8272	0.9268	0.8272	0.5542	0.2605	0.0756			
4	0.0007	0.0061	0.0315	0.1076	0.2605	0.4789	0.7057	0.8692	0.9268	0.8692	0.7057	0.4789	0.2605	0.1076

Table 2: Coefficients of $h_0(t)$, Spaced by $\frac{T}{\eta}$, for GMSK with BT= 0.3

For $\eta = 1$, the T–spaced coefficients of $h_0(t)$ are given by $\begin{bmatrix} 0.0007 & 0.2605 & 0.9268 & 0.2605 & 0.0007 \end{bmatrix}$. Neglecting the first and last coefficients, we can use a 4–state MLSE demodulator to remove the ISI introduced by $h_0(t)$.

4 Linear GMSK Demodulator

The block diagram of the proposed linearized GMSK demodulator is shown in Figure 4. The Viterbi demodulator is preceded by a *de-rotation* operation to undo the rotation performed by the GMSK modulator (c.f. 3). For an AWGN channel, a good estimate of the overall CIR is given by the 3 middle samples of $h_0(t)$, namely $\mathbf{h_0} \stackrel{def}{=} \begin{bmatrix} 0.2605 & 0.9268 & 0.2605 \end{bmatrix}$. In this paper, we assume no training overhead, therefore, the Viterbi demodulator operates in a *blind* mode and updates the CIR estimate (from its initial value of $\mathbf{h_0}$ to take the effect of $h_k(t)$ $(k = 1, 2, 3)$ into account) using its previous decisions. Finally, the output (hard) decisions of the Viterbi demodulator are differentially decoded to obtain the estimated information sequence $\hat{\alpha}_n$.

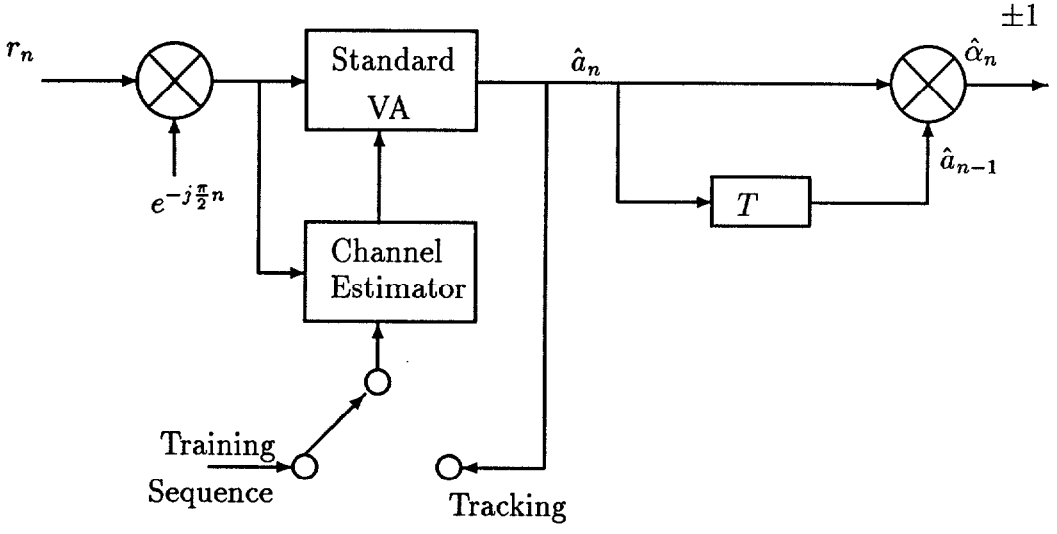

Figure 4: Proposed GMSK Demodulator

The two main disadvantages of decision–directed operation are the possibility of *error propa-*

gation and the need to recompute the locally–generated signal estimates (required to compute the VA branch metrics) every bit period based on the updated CIR. On AWGN channels, both disadvantages can be overcome, at the expense of information rate loss, by obtaining an accurate CIR estimate during a training period and holding it fixed during data demodulation (i.e. no tracking). More specifically, we cross–correlate the rotated training symbols b_n with the received noisy symbols r_n to get

$$\begin{aligned} R_l &\stackrel{def}{=} \frac{1}{N_t}\sum_{n=0}^{N_t-1} r_{n+l}b_n^* \; : \qquad\qquad \text{where } b_n = j^n a_n \\ &= \frac{1}{N_t}\sum_{n=0}^{N_t-1} \underbrace{(\sum_{k=0}^{L} j^{n+l-k}a_{n+l-k}h_k + \underbrace{v_{n+l}}_{noise})}_{r_{n+l}} j^{-n}a_n \\ &\approx \frac{1}{N_t}\sum_{k=0}^{L} j^{l-k}\underbrace{\sum_{n=0}^{N_t-1} a_{n+l-k}a_n}_{N_t\delta(l-k)}\, h_k \\ &= h_l \; : \text{ for } \textit{white} \text{ training sequence,} \end{aligned}$$

where N_t is the number of training symbols and $\delta(.)$ is the Kronecker delta function.

Remark :

For fading multipath channels, the signal component of the discrete–time received GMSK signal is given by

$$s_k \approx \sqrt{\frac{2E_b}{T}}\sum_n b_n f_{k-n}\;, \tag{3}$$

where f_k is the *overall* impulse response seen by the demodulator, i.e., it is equal to the convolution of $h_{0,k}$ with the channel impulse response and the receiver front–end filter (including any unknown frequency offsets). The coefficients f_k are determined during the training period, as described above, and can be truncated (by selecting a window of the L consecutive samples with the largest energy) to limit the complexity of the Viterbi demodulator to 2^{L-1} states. Then, this initial estimate is updated using a decision–directed LMS algorithm to track channel time variations.

5 Differential Encoding

A factor of two improvement in BER can be achieved by precoding the information sequence before passing it through the GMSK modulator. This allows us to remove the differential decoder at the receiver and make decisions based on the output of the VA, $\hat{a}_n$, directly.

It was shown in [4, 3] that

$$\begin{aligned} b_n &= j^{\sum_{k=0}^{n} \alpha_k} \\ &= j^{\alpha_n} b_{n-1} \\ &= j\alpha_n b_{n-1} \ : \text{ since } \alpha_n \in \{\pm 1\} \\ \Rightarrow \alpha_n &= \Im\{b_n b_{n-1}^*\} \ . \end{aligned} \tag{4}$$

This shows the *double-error* characteristic of GMSK modulation. To convert double errors to single errors, we use the following precoding rule at the transmitter

$$\alpha_n = a_n a_{n-1} \ , \tag{5}$$

i.e., $a_n \in \{\pm 1\}$ is the information sequence in this case. Combining Equation (4) with (5) we have

$$\begin{aligned} b_n &= j a_n a_{n-1} b_{n-1} \\ &= (j a_n a_{n-1})(j a_{n-1} a_{n-2} b_{n-2}) \\ &= (j a_n a_{n-1})(j a_{n-1} a_{n-2}) \cdots (j a_1 a_0 b_0) \\ &= j^n a_n a_0 b_0 = \pm j^n a_n \ , \end{aligned}$$

in agreement with (3). Therefore, an estimate of the transmitted data sequence, $\hat{a}_n$, is available at the output of the Viterbi demodulator and we can eliminate the differential decoder.

6 Simulation Results

The proposed GMSK demodulator was simulated using SPW© to evaluate its performance. Block diagrams of the SPW© implementation are shown in Figures 5 and 6. We simulated the 4–state linearized Viterbi demodulator in AWGN under 2 scenarios. In the first scenario, the CIR estimate is *fixed* at $h_0(t)$ while in the second scenario it is updated using a decision–directed LMS algorithm. Note that under both scenarios, we perform *blind* demodulation in the sense that no training signal is used. The results are depicted in Figure 7. For comparison, we have also included BER curves for coherent symbol–by–symbol detection [5] and for MSK. It is clear that the adaptive 4–state MLSE demodulator achieves optimal performance (same as MSK).[1]

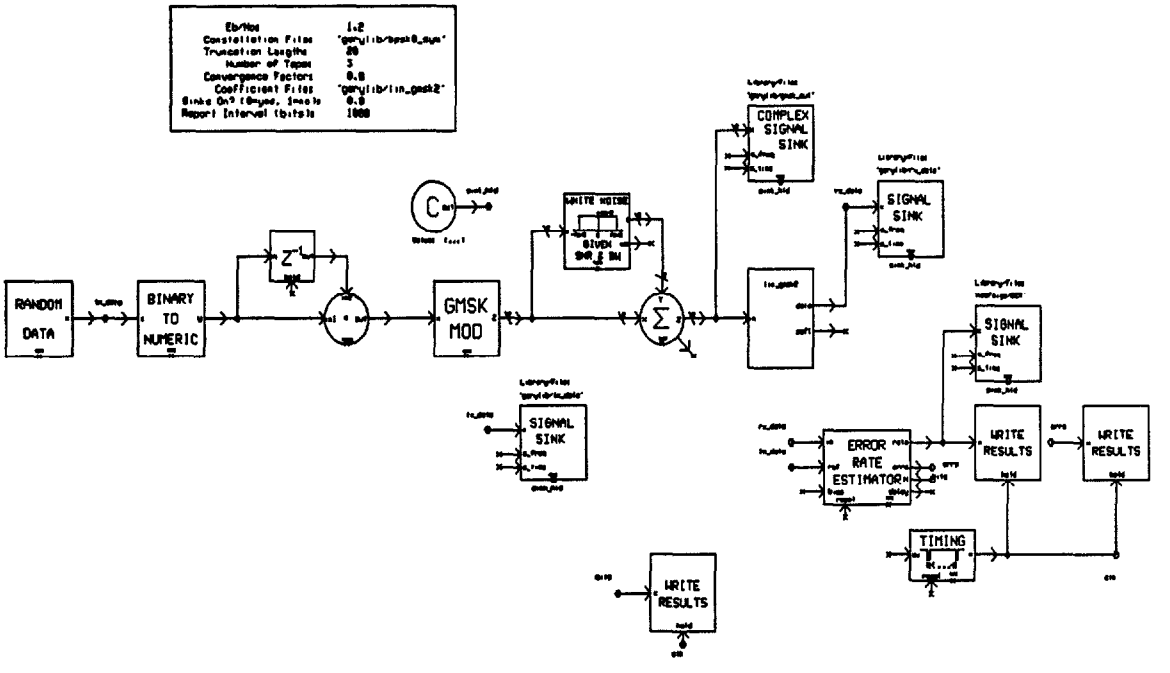

Figure 5: Block Diagram of the SPW© Implementation

[1]The slight performance degradation at high $\frac{E_b}{N_0}$ is mainly due to the effect of $h_1(t)$, which was ignored in our linear approximation. This loss can be reduced by obtaining a better CIR estimate that takes $h_1(t)$ into account.

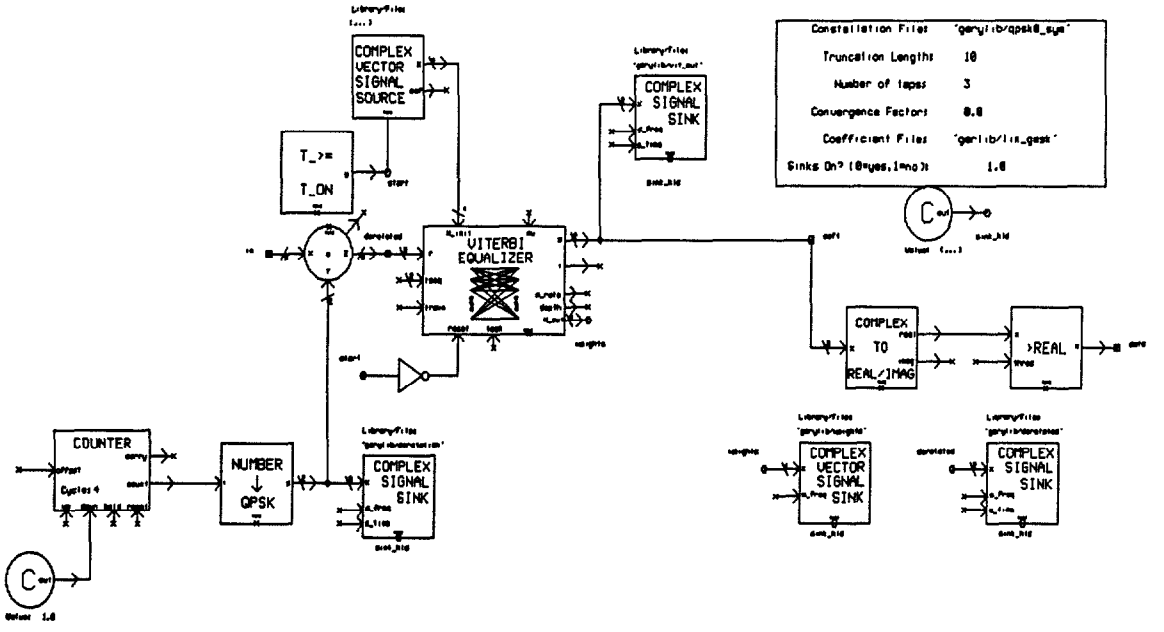

Figure 6: Block Diagram of the Proposed Linearized GMSK Demodulator

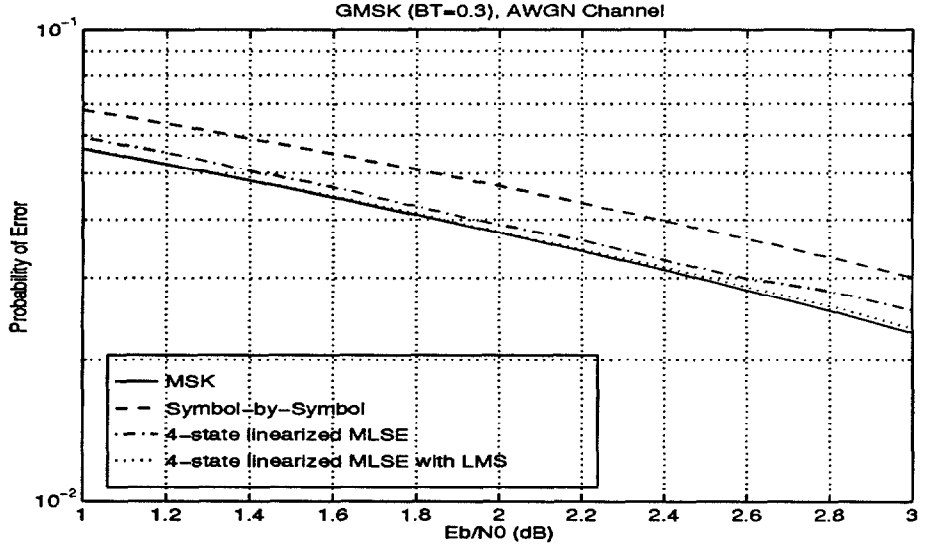

Figure 7: BER Performance Comparison between Two Implementations of the Linearized GMSK Demodulator (with and without Adaptation) and Both Coherent Symbol-By-Symbol Detection and Ideal MSK

7 Conclusions

In this report, we described and simulated a 4–state symbol–spaced adaptive MLSE GMSK demodulator that achieves optimum BER performance (same as MSK) on AWGN channels. A near–optimum CIR estimate is derived analytically and used to initialize the decision–directed adaptive MLSE, thus avoiding any training overhead. The linear nature of the demodulator allows us to use a standard off–the–shelf Viterbi processor.

References

[1] J. Anderson, T. Aulin, and C. Sundberg. *"Digital Phase Modulation"*. Plenum, 1986.

[2] G.D. Forney Jr. "Maximum-Likelihood Sequence Estimation of Digital Sequences in the Presence of Intersymbol Interference". *IEEE Transactions on Information Theory*, 18(3):363–378, May 1972.

[3] G.K. Kaleh. "Simple Coherent Receivers for Partial Response Continuous Phase Modulation". *IEEE Journal on Selected Areas in Communications*, 7(9), December 1989.

[4] P. Laurent. "Exact and Approximate Construction of Digital Phase Modulations by Superposition of Amplitude Modulated Pulses (AMP)". *IEEE Trans. on Communications*, 34(2):150–160, February 1986.

[5] K. Murota, K. Kinoshita, and K. Hirade. "GMSK Modulation for digital mobile telephony". *IEEE Trans. on Communications*, 29:1044–1050, July 1981.

[6] R. Steele. *"Mobile Radio Communications"*. Pentech Press, 1995.

N. Al-Dhahir
G. Saulnier

A High-Performance Reduced-Complexity GMSK Demodulator

96CRD107
September 1996